

MATHEMATICAL MODELLING OF PATTERN SUBLIMATION IN RAPID ICE INVESTMENT CASTING

Rajendra Hodgir , **Yash Gopal Mittal**, **Pushkar Kamble**, **Gopal Gote**, and **K. P. Karunakaran**
Indian Institute of Technology Bombay, Powai, Mumbai 400076, India

Yogesh Patil and **Ashik Kumar Patel**
National Institute of Industrial Engineering (NITIE), Vihar Lake, Mumbai 400087, India

Alain Bernard
Ecole Centrale de Nantes, Rue de la Noë, 44300 Nantes, France

Copyright © 2021 American Foundry Society
<https://doi.org/10.1007/s40962-021-00665-w>

Abstract

Investment Casting (IC), using the wax pattern, produces metal parts with a high surface finish and complex geometries within acceptable tolerances. However, removing the wax patterns can have processing challenges, such as thermal expansion during wax melting for pattern removal leading to shell cracking defects, the release of hydrocarbons from melting wax, and the burnt residue from this process. To overcome these challenges, it has been proposed to replace wax with ice as a pattern material. Ice has an inherent benefit of reduction of volume during its phase change from solid to liquid. It helps to reduce cracking due to expansion. Rapid Freeze Prototyping (RFP) and Freeze Cast Process (FCP) can produce the ice pattern. In the process of Rapid Ice Investment Casting (RIIC), the ice pattern is invested with a low-temperature ceramic slurry to make ceramic shells for

metal casting. Sublimation is used for ice pattern evacuation at sub-zero conditions using a vacuum. Estimating various properties like time for total sublimation, concentration gradient, and energy usage are vital for process characterization and optimization. A diffusion-based mathematical model has been proposed and experimentally verified to sublimate the ice patterns in this research. Experimental results show a close correlation (96.74%) with the theoretical model. The demonstration of ice investment casting has been carried out, and it reported close dimensional accuracy.

Keywords: ice pattern, rapid freeze foundry, diffusion, ice sublimation, freeze drying

Introduction

The casting industry is an essential subdivision of the manufacturing sector to produce intricate shapes with close tolerance. Among several casting processes like die casting, sand casting, plaster mould casting, semi-solid die casting and squeeze casting, investment casting is a superior manufacturing process with no metallurgical limitations.¹ Investment casting is a process by which intricately shaped wax patterns are transformed into solid metal parts

with close tolerance by succeeding a multi-step process.² Researchers have also used other manufacturing processes such as indirect additive manufacturing, for designing and fabrication of complex structure castings.³⁻⁵

Wax is the most commonly used pattern material, but several kinds of polymeric foam such as polyurethane (PU) and expandable polystyrene foam (EPS) and stereolithography patterns are also used for investment casting.⁶

The wax patterns exhibit volumetric expansion as it starts to melt during dewaxing, leading to the severe problem of shell cracking.⁷ Moreover, the weight and brittleness of the

wax pattern lead to problems like handling and distortion during storage.⁸ Compared to the wax pattern, polymeric foam reported a more significant coefficient of thermal expansion, which leads to more tendency of shell cracking while pattern removal.⁹

Innovative methods to augment the performance of investment casting are repetitively being pursued. A novel investment casting method, called the Rapid Ice Investment Casting (RIIC), is developed by replacing wax patterns with ice patterns. Freeze cast process (FCP) and Rapid freeze prototyping (RFP) are two proposed ways for producing ice patterns for RIIC. The FCP was invented by Yodice¹⁰ and has proved the suitability of investment casting with ice patterns.^{11–13} In FCP, the master pattern is 3D printed and then used to create a silicon rubber mould. The final ice pattern is obtained by freezing the water in the silicon rubber mould. The predominant merits of FCP are good surface finish, high quality, and low cost making it an ideal substitute for the investment casting process.¹³

When it comes to the intricate ice pattern, RFP is the process in which ice pattern is fabricated from a CAD model by freezing water droplets, layer by layer.^{14–16} RFP provides better accuracy and more flexibility in designing and modelling ice patterns. Since ice is the pattern material, the moulding process has to occur at sub-zero temperatures. Therefore, the mould material is different from the traditional one and must exhibit its flowability properties and retain the shape even at sub-zero conditions. In the process of ice investment casting, the slurry is poured over the ice pattern. As with conventional investment casting, the ice pattern needs to be removed from the ceramic mould to obtain the mould cavity in a controlled process. Solid-state-evaporation (sublimation) is the proposed solution for mould evacuation to get the required dimensional accuracy without disturbing the mould cavity's intricacies. Lyophilization or freeze-drying is a process in which the removal of ice is done by the sublimation process.¹⁷ A condensation device collects the sublimated water, and it is discarded after the lyophilization operation. After a complete sublimation of the ice pattern, the ceramic mould is fired around 900 °C for four hours to withdraw the trapped moisture and cure the shell. Mingzhi Xu et al. used firing temperatures of range 850–1000 °C for different material coats.¹⁸ Finally, the cast part is obtained by pouring the molten metal into the mould and knockout after solidification.

It is necessary to develop a relationship for the sublimating ice mass with respect to time. Various researchers came up with several mathematical models on ice sublimation for multiple applications. Kossacki et al. studied the sublimation rate on the surfaces homogeneously covered with the non-volatile granular materials and considered the effect of the characteristic pore radius and non-volatile layer thickness over the ice surface.¹⁹ Chevrier studied the ice

sublimation rate under-stimulated Martian conditions at sub-zero and sub-atmospheric conditions.^{20,21} Kumar studied and characterized ceramic shells in investment casting process for enhancing properties such as permeability using fillers.^{22,23} Numerical tools and simulations can also be used to determine optimal process parameters for investment casting.²⁴

In this research, a novel mathematical model based on diffusion phenomena is presented to sublimate the ice patterns. The model delivers an explicit equation relating to ice mass variation with respect to the elapsed time. Various physical factors, such as the thickness of the non-volatile substrate layer, diffusion conditions of the ice-water system, starting geometry of the sublimating ice pattern, etc., are considered in devising the correlation. Physical experiments were conducted using the lyophilization process to evacuate the ice pattern from the ceramic mould. Experimental results exhibit a close correlation with the proposed theoretical model. The model can predict multiple interlinked properties such as concentration gradient, diffusive mass-flux, overall heat exchange, power requirement, etc. These can be used in various domains such as jewellery, rapid ice casting, freeze drying, food processing, etc.

Mathematical Model

Based on Fick's law of diffusion, a mathematical model for the sublimation of ice was theorized. Diffusion, described as the constituent entities' overall movement across regions of varying concentration gradient, follows Fick's law. Fick's law relates the diffusive flux (flow of entities per unit area per unit time) to the concentration gradient (Eqn. 1). The flux magnitude is proportional to the concentration gradient, measured in the direction of flow from a higher concentration level to a relatively lower concentration. A proportionality constant, called the diffusion coefficient, D , is present to preserve the dimensionality. Mathematically,

$$J = D \frac{dC}{dx} \quad \text{Eqn. 1}$$

where J is the diffusive flux, D is the diffusion coefficient (m^2/s), C is the concentration of the constituent entities, x is the direction of flux flow, and $\frac{dC}{dx}$ is the concentration gradient.

A similar approach is presented where the concentration gradient is described in terms of the instantaneous ice mass (M) present inside the semi-solidified mould cavity and the average distance of the ice mass from the free surface of the slurry (L) (Eqn. 2). Mathematically,

$$\frac{dC}{dx} = \frac{M}{L} \quad \text{Eqn. 2}$$

The flux multiplied by the instantaneous mass-transfer surface area will give a measure of the instantaneous rate of change of ice mass ($\frac{dM}{dt}$). A solid spherical ice body of initial mass and radius as M_o and R_o respectively is considered for the modelling. A spherical geometry has the minimal surface-area to volume ratio for a given mass. The convex geometry of a sphere presents a gradually changing normal vector field over the inclination. Thereby changing the flux transfer at every height segment, offering a challenging analysis. The ice mass is covered with slurry from all sides, maintaining an initial average non-volatile layer of L_o , measured between the top/free surface of the slurry and the ice-mass centre at the start ($t = 0$), as shown in Fig. 1.

The initial flux can be calculated using Eqn. 3,

$$\frac{dM}{dt} = kA_o \frac{M_o}{L_o} \quad \text{Eqn. 3}$$

where k ($m^{-1} s^{-1}$) is the modified diffusion coefficient, given as $\frac{D}{V_m}$, with V_m as the molar volume of the solvent; and A_o is the initial diffusive surface area ($4\pi R_o^2$).

With time ($t > 0$), the ice mass will sublime, causing associated mass and volume reduction. It is assumed that the ice mass will settle down under gravity, maintaining its sphericity. Generally, the slurry undergoes gelation process once it is poured on the ice pattern²⁵, thereby the slurry's dimensional integrity will not change, and the following relation (Eqn. 4) can be made,

$$L_o + R_o = L_f + R_f \quad \text{Eqn. 4}$$

L_f and R_f are the average non-volatile layer thickness and radius of the ice mass at a time (t), as shown in Fig. 2.

The variation of ice mass with time can be calculated by solving the first-order, homogeneous differential equation. The mathematical relation is given in Eqn. 5,

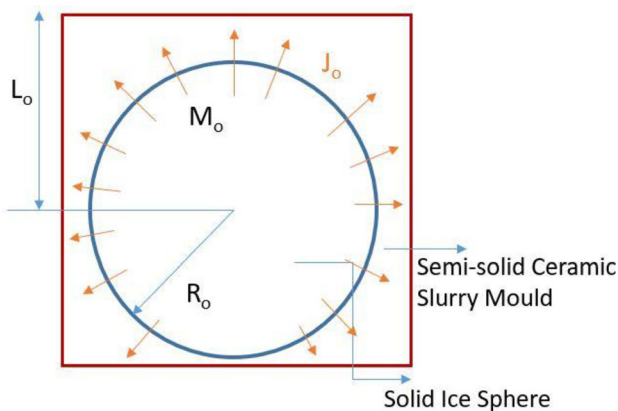


Figure 1. Schematic of the diffusion-based sublimation of ice.

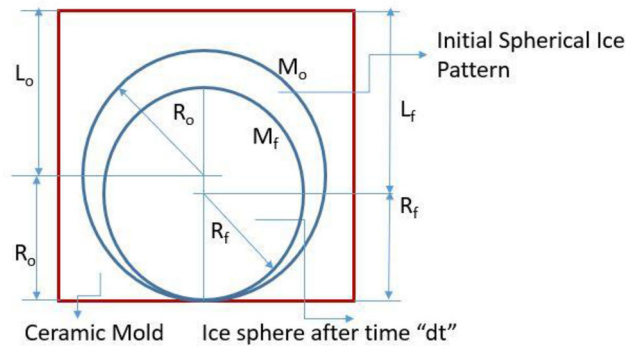


Figure 2. Schematic of the variation of ice-mass and non-volatile layer with time.

$$\frac{dM}{dt} = kA_f \frac{M(t)}{L_f} = \frac{k4\pi R_f^2 M(t)}{L_o + R_o - R_f} \quad \text{Eqn. 5}$$

The relation between the instantaneous radius of the ice sphere (R_f) and its mass is given in Eqn. 6,

$$R_f = \left(\frac{3M(t)}{4\pi\rho} \right)^{\frac{1}{3}} \quad \text{Eqn. 6}$$

where ρ is the density of the ice mass. Putting the values of Eqn. 6, in Eqn. 5 and solving the differential equation with the initial condition, $M(0) = M_o$, yields,

$$\begin{aligned} & \frac{3}{M(t)^{\frac{1}{3}}} \left\{ 1 - 0.5 \left[\left(\frac{M_o}{M(t)} \right)^{\frac{1}{3}} + \frac{L_o}{\left(\frac{3M(t)}{4\pi\rho} \right)^{\frac{1}{3}}} \right] \right\} \\ & = \left\{ 4\pi \left(\frac{3}{\rho} \right)^{\frac{2}{3}} kt \right\} + \frac{3}{M_o^{\frac{1}{3}}} \left\{ 1 - 0.5 \left[1 + \frac{L_o}{\left(\frac{3M_o}{4\pi\rho} \right)^{\frac{1}{3}}} \right] \right\} \end{aligned} \quad \text{Eqn. 7}$$

Equation 7 can be solved in $M(t)$ to yield an explicit form, depending only on time, for given conditions of the mould cavity, operating pressure & temperature, slurry composition, etc. The final equation was a time-dependent relationship with the sublimating ice-mass, with the dependence of temperature and vacuum indirectly considered within k , in terms of D and V_m . The effect of slurry permeability was not considered as the ceramic slurry was a water-based colloidal silica solution with uniformly dispersed ceramic powder. Hence, the diffusive mass transfer coefficient of water (D) was directly used.

Materials for Ice Investment Moulding

Various researchers have found that the material used in ice investment casting has different properties from traditional wax-based investment casting.²⁶ The slurry, being at sub-zero conditions, should not solidify before entering the mould's intricate parts. The primary materials for mould preparation in RIIC are ceramic powder, binder, and catalyst.

Ceramic

The slurry's main constituents are ceramic powder and binder, playing a vital role in the mould-making process. Commonly, ceramic materials are used in various blends and include aluminosilicates, silica sand, fused silica, alumina, and zirconium silicate. Selecting the appropriate set of ceramic materials is required to get high dimensional accuracy, smooth surface finish, and sound metal castings. Liu et al.¹³ used alumino-silicates of grain size 200 mesh with reinforced fused silica. The fine ceramic powder was used to make the mould for applications such as dentistry.²⁶

Binder

Binder is another vital slurry material that is used with ceramic powder. In RIIC, the binder should hold good fluidity and binding strength. These are the general requirement while choosing the binder material. In general, silica gel, water glass, and ethyl silicate can be used as binder materials. Silica sol (particles of Silica are uniformly dispersed in water to make colloidal solution) is an environment-friendly binder in metal casting.²⁷ Liu et al. used alcohol-based pre-hydrolysed ethyl silicate with 18% silica by weight as binder material.²⁶

In this work, as a part of the study, a new slurry material was developed using plaster of Paris as the ceramic material and 30% colloidal silica, by weight, as the binder. The composition of the slurry material is mentioned in Table 1. The composition is selected based on the preliminary experiments. It has the advantage of quick gelling and setting time of 15–20 s.

Table 1. Composition of the Slurry Material

Sr. no.	Component	Quantity
1	Plaster of Paris	100 gm
2	Colloidal silica (30% by weight dissolved in water)	50 ml

Experimental Methodology

The process of RIIC starts with the CAD model of the desired part. The CAD is then converted into an ice pattern. The process flowchart of RIIC is shown in Fig. 3. In the present research, FCP was used to fabricate the ceramic mould cavity.

A master pattern is fabricated, which is used to obtain the silicon rubber mould. The rubber mould is filled with distilled water and allowed to freeze to get the ice pattern. Simultaneously, the mould flask and slurry constituents like ceramic powder and colloidal silica should be pre-cooled to bring down the thermal gradient and temperature difference with respect to the ice pattern. The ice pattern is kept inside the mould flask and poured over with the pre-cooled slurry. The mould is allowed to solidify with the submerged ice pattern and then transferred into the Lyophilizer.

Lyophilization, also known as freeze-drying, is a technique in which the frozen water is made to sublimate by lowering the temperature and pressure. The chamber environment of the Lyophilizer must be maintained below the triple point

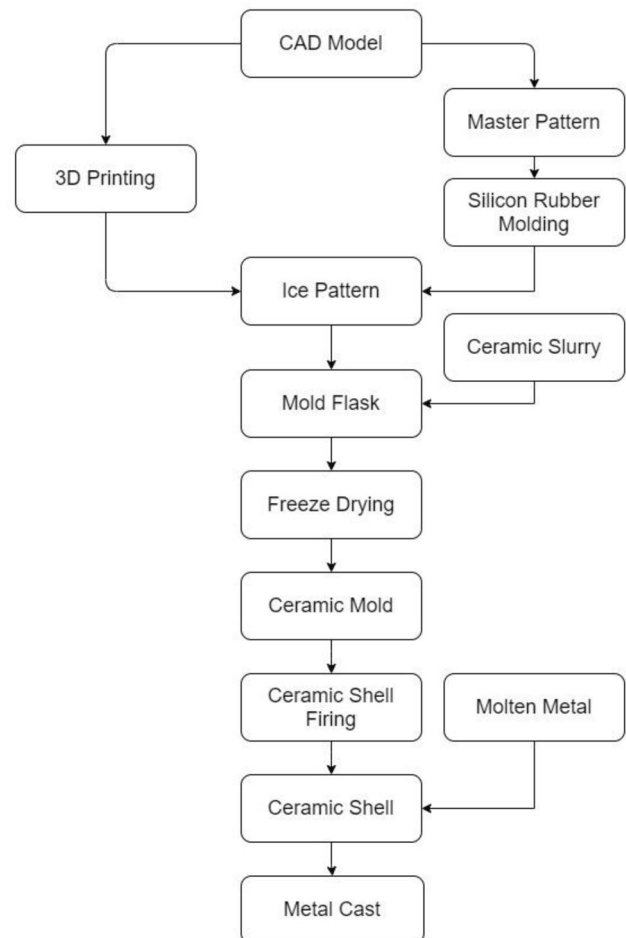


Figure 3. Flowchart of rapid ice investment casting.

of water (0.0075 °C and 4.55 mm Hg) to sublimate the ice pattern. The Lyophilization system is used for the sublimation of ice pattern. A schematic of the Lyophilizer is shown in Fig. 4. Initially, the ice mass is kept at $-5\text{ }^{\circ}\text{C}$ at normal atmospheric pressure and is finally made to sublimate by shifting inside Lyophilizer.

Complete sublimation of ice pattern provides the ceramic mould. Any remaining water content from the mould cavity is removed, and shell curing is achieved by exposing the ceramic mould to $900\text{ }^{\circ}\text{C}$ for four hours in a burn-off furnace. Molten metal is then poured into the mould cavity and is allowed to solidify. After complete solidification, the mould is broken open to get the casted part of the geometry.

An FDM 3D printed spherical model of 30 mm diameter, as shown in Fig. 5a, is used as the master pattern. The master pattern of ABS plastic is printed on the Stratasys uPrint Dimension series printer. The standard layer height of 0.254 mm is used. The corresponding silicon rubber mould is obtained Fig. 5b.

The ice pattern shows the increase in the average diameter since the ice tends to expand during solidification by approximately 4% by volume. The final dimension of the metal casted part is observed as 30.11 mm. The reason for the reduction in the diameter is the shrinkage that occurred during the solidification of the metal. The comparison between FDM model, ice pattern and metal casted part, is mentioned in Table 2.

The ice pattern, Fig. 5c, is obtained by pouring distilled water into the silicon mould and freezing completely. Simultaneously, the ceramic powder, binder and mould flask are pre-cooled to reduce the thermal difference with respect to ice pattern, as shown in Fig. 5d. The ceramic slurry is prepared using 200 g gypsum powder mixed with 100 ml colloidal silica as the binder material.

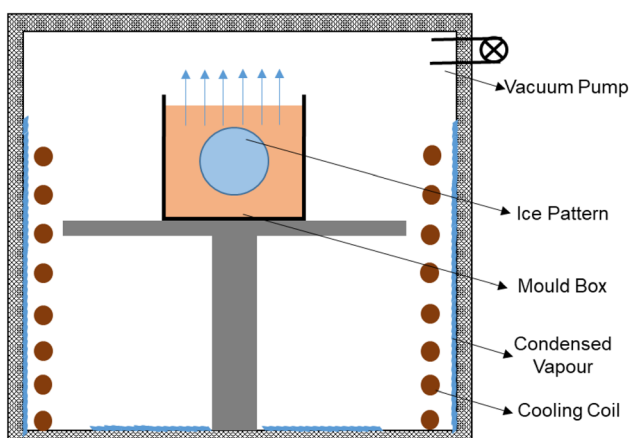


Figure 4. Schematic diagram of the Lyophilizer.

The pre-cooled slurry is then poured over the ice pattern and transferred into the Lyophilizer to obtain the mould cavity by sublimating the ice pattern.

The lyophilization system of the company Martin Christ is used. The ice mass is initially kept at sub-zero conditions ($-5\text{ }^{\circ}\text{C}$) at normal atmospheric pressure and is finally made to sublimate at $-50\text{ }^{\circ}\text{C}$ and 0.75 mm Hg pressure, as shown in Fig. 6.

The ceramic mould is obtained after the complete sublimation of the ice pattern. The mould is fired to remove any remaining water content from it. For simplicity of the melting and casting, a lead-tin alloy is selected to prove the concept. A lead-tin alloy is melted and poured into the mould cavity and is allowed to solidify. The mould is break-open to get the casted part of the spherical geometry, as shown in Fig. 5e. The obtained casting is dimensionally accurate and spherical in nature, with a mean diameter of 30.11 mm, as shown in Fig. 5f.

Results and Discussions

A solid ice spherical pattern of 13 g initial mass (M_o) was fabricated for the experimental analysis. The corresponding radius (R_o) was 15 mm ($\rho_{\text{ice}} = 920\text{ kg/m}^3$).²⁸ The slurry layer above the ice sphere was kept at 2 mm, giving the initial average slurry layer (L_o) of 17 mm, as measured from the centre of the spherical ice pattern. The modified diffusion coefficient (k) was calculated for water with Fick's diffusion coefficient (D) as $1.8 \times 10^{-6}\text{ m}^2/\text{s}$ and molar volume (V_m) of 18 cubic centimetres.²⁹ The resulting relation of the variation of ice-mass with time, as determined using Eqn. 8, was

$$M(t) = \left(\frac{\sqrt{10.8944 + 1.63626 \times 10^{-4} \times t} - 3}{1.28 + 1.513 \times 10^{-4} \times t} \right)^3 \quad \text{Eqn. 8}$$

It is observed that there is a close correlation between analytical values and the experimental results. The initial ice mass reduction rate is higher because of the high thermal gradient and large surface area. The relation correctly estimates the initial mass of 13 g and asymptotically touches the x-axis (time), as shown in Fig. 7. Hence, to estimate the total sublimation time, a lower bound on ice mass can be a fraction of the initial mass set as per requirement. In this work, the authors considered the lower bound as 10% of initial mass, i.e., 1.3 g, and the time reported for it was 66 h (roughly three days). Generally, shell preparation for the investment casting takes around 5–6 days.³⁰ The given process shortens the time to 3 days.

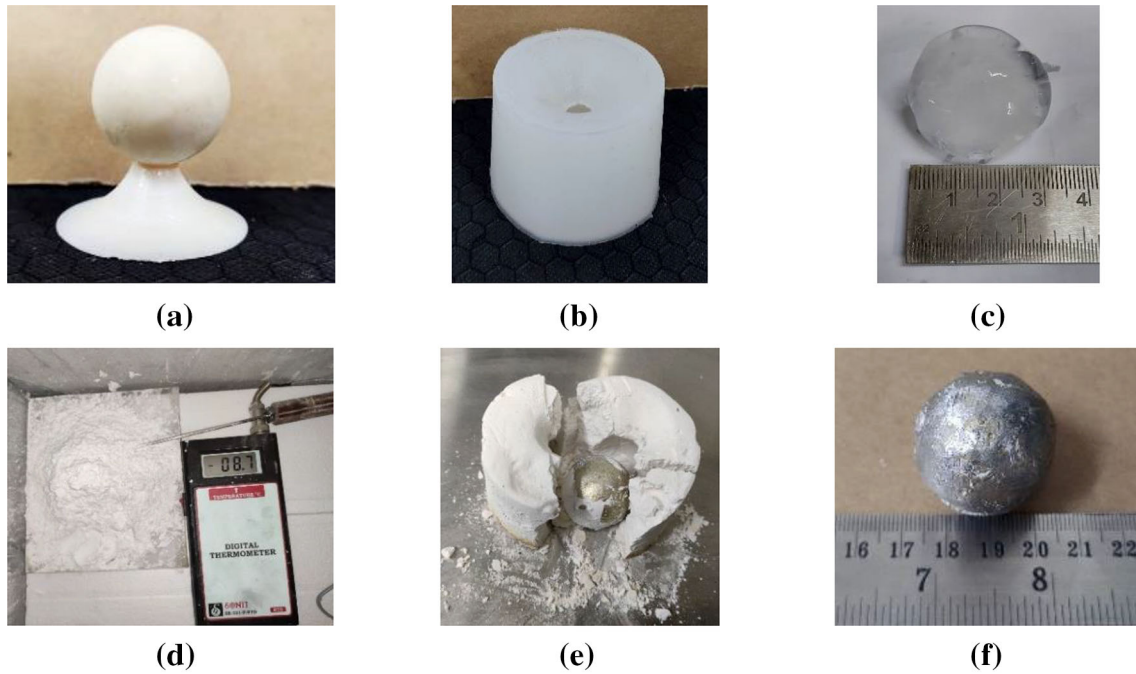


Figure 5. Photographs of RIIC: (a) FDM Master Pattern, (b) Silicon Rubber Mould, (c) Ice Pattern, (d) Ceramic Powder, (e) Fettling and (f) Metal Casted Part.

Table 2. Comparison Between FDM Model, Ice Pattern and Metal Casted Part

Stage	FDM master pattern	Ice pattern	Metal casted part
Average diameter	30.05 mm	31.20 mm	30.11 mm

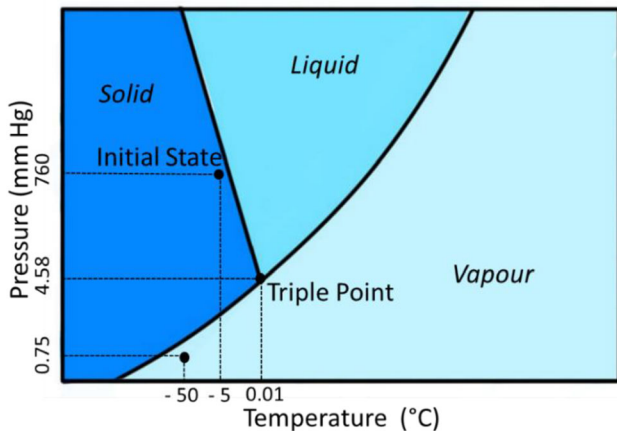


Figure 6. Initial and final states mentioned over the phase diagram of water.

The mass of the spherical ice pattern was measured at various time intervals using a digital weighing scale. The measured values are given in Table 3.

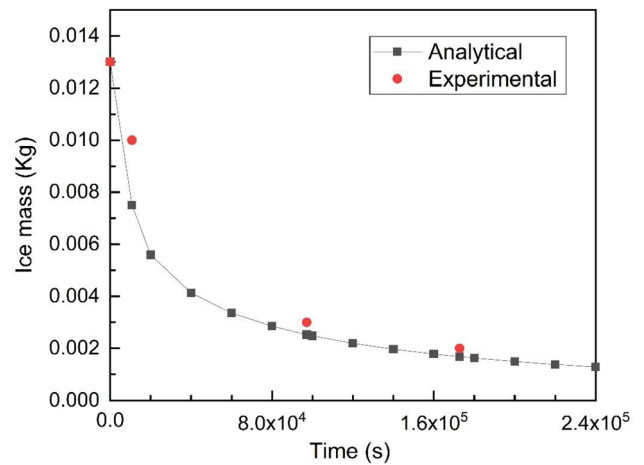


Figure 7. Variation of ice-mass with respect to time.

Table 3. Variation of Ice Pattern Mass with Time

Time (h)	Mass of spherical ice pattern (g)
0	13
3	10
27	3
48	2

Correlation Analysis

A mathematical correlation between the experimental and the predicted values were determined to estimate the

model's effectiveness. The experimental values were treated as independent variables. The analytical values devised from the proposed model (using Eqn. 8) for the experimental ones' corresponding time duration were treated as the dependent variable, as shown in Table 4.

The standard two-variable correlation (Eqn. 9) was used to determine the correlation coefficient (r).

$$r = \left(\frac{1}{n-1} \right) \sum \left(\frac{x - \mu_x}{\sigma_x} \right) \left(\frac{y - \mu_y}{\sigma_y} \right) \quad \text{Eqn. 9}$$

where n is the number of x - y pairs (4, here), x & y are the independent and dependent variables respectively, μ & σ are the mean and standard deviation, respectively, of the associated variables. Table 5 depicts the mean and standard deviations for independent and dependent values.

The correlation coefficient estimated using Eqn. 9 came out to be 0.96739, indicating a positive correlation of about 96.7% between the experimental and analytical values.

Table 4. Experimental and Analytical Values of the Ice Mass for the Corresponding Time Durations

Sr. no.	Experimental values of the ice-mass (kg)	Corresponding time duration (h)	Analytical values of the ice-mass (kg) for corresponding time duration (h)
1	0.013	0	0.012961
2	0.010	3	0.007033
3	0.003	27	0.002525
4	0.002	48	0.001677

Table 5. Mean and Standard Deviations for the Various Independent and Dependent Values

i	1	2	3	4	Mean (μ)	SD (σ)
Independent Values (x)	0.013	0.010	0.003	0.002	0.007	0.005354
Dependent Values (y)	0.012961	0.007033	0.002525	0.001677	0.006049	0.005173

Conclusion

The model presented in this study closely predicts the variation of sublimating ice mass with respect to time. The model delivers a diffusion-based sublimating ice mass transfer model, solved explicitly from a first-order homogeneous differential equation. The presented paradigm shows an asymptotic behaviour with time, as a result of which a lower bound for the sublimating ice mass has to be set to cut off the process. The high initial sublimating mass transfer can be treated due to the large concentration gradients and surface area available at the start. The predicted model is advantageous in various manufacturing processes such as RIIC, where an ice pattern replaces the traditional wax pattern. The mould-making process requires the removal of ice patterns without disturbing the ceramic mould's geometry. The sublimation route for ice pattern elimination is the most favourable as it directly converts the ice mass into its vapour state. The demonstration of ice investment casting is carried out. The casted spherical part reported a 30.11 mm average diameter compared to the 31.2 mm diameter of the ice pattern.

As a part of the future investigation, properties such as concentration gradient, pattern shape integrity, total mass transfer, energy requirement & power consumption, etc., can be determined analytically using the described model.

Acknowledgements

The authors wish to acknowledge the help extended by the Department of Chemical Engineering, IIT Bombay, regarding experimental work.

Funding

There are no financial conflicts of interest to disclose.

Availability of data and material

Not applicable.

Code availability

Not applicable.

Declarations

Conflicts of interest Not applicable.

Ethics approval Not applicable.

Consent to participate Not applicable.

Consent for publication Not applicable.

REFERENCES

1. S. Kumar, D.B. Karunakar, *Int. J. Met.* **15**, 98–107 (2021). <https://doi.org/10.1007/s40962-020-00421-6>
2. M.P. Groover, *Fundamentals of Modern Manufacturing*, 4th edn. (Wiley, Hoboken, 2010), pp. 225–253
3. D. Almonti, N. Ucciardello, *Materials* **12**, 2261–2274 (2019). <https://doi.org/10.3390/ma12142261>
4. D. Almonti, G. Baiocco, V. Tagliaferri, N. Ucciardello, *Materials* **13**, 1085–1096 (2020). <https://doi.org/10.3390/ma13051085>
5. D. Almonti, G. Baiocco, E. Mingione, N. Ucciardello, *Int. J. Adv. Manuf. Technol.* **111**, 1157–1172 (2020). <https://doi.org/10.1007/s00170-020-06092-1>
6. C. Liu, F. Wang, S. Jin, F. Li, X. Lai, *Int. J. Met.* **13**, 953–968 (2019). <https://doi.org/10.1007/s40962-019-00317-0>
7. Druschitz EA. Investment shell cracking. Missouri University of Science and Technology; 2009. https://scholarsmine.mst.edu/masters_theses/5003. Accessed 20 June 2020
8. H. Zhao, P.K. Nam, V.L. Richards, S.N. Lekakh, *Int. J. Met.* **13**, 18–25 (2019). <https://doi.org/10.1007/s40962-018-0240-5>
9. W. Everhart, S. Lekakh, V. Richards, J. Chen, H. Li, K. Chandrashekhara, *Int. J. Met.* **7**, 21–27 (2013). <https://doi.org/10.1007/BF03355541>
10. Yodice DB. U. S. Patent 5,072,770, 17 Dec 1991
11. Q. Liu, M.C. Leu, *Int. J. Adv. Manuf. Technol.* **29**, 317–335 (2006). <https://doi.org/10.1007/s00170-005-2523-2>
12. Liu Q, Leu MC. In: International solid freeform fabrication symposium, 2004. <https://doi.org/10.26153/tsw/7025>
13. Q.B. Liu, M.C. Leu, V.L. Richards, *Int. J. Cast Met. Res.* **20**, 14–24 (2007). <https://doi.org/10.1179/136404607X202708>
14. M.C. Leu, Q. Liu, F.D. Bryant, *CIRP Ann.* **12**, 185–188 (2003). [https://doi.org/10.1016/S0007-8506\(07\)60561-7](https://doi.org/10.1016/S0007-8506(07)60561-7)
15. L. Qingbin, G. Sui, M.C. Leu, *Comput. Ind.* **48**, 181–197 (2002). [https://doi.org/10.1016/S0166-3615\(02\)00042-8](https://doi.org/10.1016/S0166-3615(02)00042-8)
16. P. Kamble, S. Chavan, K.P. Karunakaran, *J. Emerg. Technol.* **5**, 119–131 (2018)
17. J.C. Kasper, G. Winter, W. Friess, *Eur. J. Pharm. Biopharm.* **85**, 162–169 (2013). <https://doi.org/10.1016/j.ejpb.2013.05.019>
18. M. Xu, S.N. Lekakh, V.L. Richards, *Int. J. Met.* **10**, 329–337 (2016). <https://doi.org/10.1007/s40962-016-0052-4>
19. K.J. Kossacki, K. Misiura, L. Czechowski, *Icarus* **329**, 72–78 (2019). <https://doi.org/10.1016/j.icarus.2019.03.019>
20. V. Chevrier, D.R. Ostrowski, D.W.G. Sears, *Icarus* **196**, 459–476 (2008). <https://doi.org/10.1016/j.icarus.2008.03.009>
21. V. Chevrier, D.W.G. Sears, J.D. Chittenden, L.A. Roe, R. Ulrich, K. Bryson, L. Billingsley, J. Hanley, *Geophys. Res. Lett.* **34**, 3–7 (2007). <https://doi.org/10.1029/2006GL028401>
22. S. Kumar, D.B. Karunakar, *Int. J. Met.* **13**, 588–596 (2019). <https://doi.org/10.1007/s40962-018-00297-7>
23. S. Kumar, D.B. Karunakar, *Int. J. Met.* **15**, 98–107 (2020). <https://doi.org/10.1007/s40962-020-00421-6>
24. Z.H. Wang, J. Wang, B. Yu, J. Wu, M. Wang, B. Su, *Int. J. Met.* **13**, 74–81 (2019). <https://doi.org/10.1007/s40962-018-0228-1>
25. G. Dietler, C. Aubert, D.S. Cannell, P. Wiltzius, *Phys. Rev. Lett.* **57**, 3117–3121 (1986)
26. Q. Liu, M.C. Leu, V.L. Richards, S.M. Schmitt, *Int. J. Adv. Manuf. Technol.* **24**, 485–495 (2004). <https://doi.org/10.1007/s00170-003-1635-9>
27. Y. Jing, L. Dehong, W. Zhao, J. Yehua, *Int. J. Met.* **9**, 4 (2015). <https://doi.org/10.1007/BF03356038>
28. T. Watts, C. Derksen, C.C. Canada, M. Sandells, *Cryosphere* **9**, 5979–6002 (2015). <https://doi.org/10.5194/tcd-9-5979-2015>
29. K. Goto, T. Hondoh, A. Higashi, *Jpn. J. Appl. Phys.* **25**, 351–357 (1986). <https://doi.org/10.1143/JJAP.25.351>
30. S. Pattnaik, D.B. Karunakar, P.K. Jha, *J. Mater. Process. Technol.* **212**, 2332–2348 (2012). <https://doi.org/10.1016/j.jmatprotec.2012.06.003>

Publisher's Note Springer Nature remains neutral with regard to jurisdictional claims in published maps and institutional affiliations.